

IMF isotopic properties in semi-peripheral collisions at Fermi energies

R.Lionti, V.Baran*, M.Colonna, M. Di Toro
*Laboratori Nazionali del Sud INFN,
Phys.Astron. Dept. Catania University
Via S. Sofia 62,
I-95123 Catania, Italy
E-mail: ditoro@lns.infn.it*

We study the neutron and proton dynamical behavior along the fragmentation path in semi-peripheral collisions: $^{58}\text{Fe}+^{58}\text{Fe}$ (charge asymmetric, $N/Z = 1.23$) and $^{58}\text{Ni}+^{58}\text{Ni}$ (charge symmetric, $N/Z = 1.07$), at 47 AMeV. We observe that isospin dynamics processes take place also in the charge-symmetric system $^{58}\text{Ni}+^{58}\text{Ni}$, that may produce more asymmetric fragments. A neutron enrichment of the neck fragments is observed, resulting from the interplay between pre-equilibrium emission and the phenomenon of *isospin-migration*. Both effects depend on the *EoS* (Equation of State) symmetry term. This point is illustrated by comparing the results obtained with two different choices of the symmetry energy density dependence. New correlation observables are suggested, to study the reaction mechanism and the isospin dynamics.

PACS numbers: 25.70-7, 21.30.Fe, 24.10.Cn, 21.65.+f

Keywords: neck fragmentation, isospin transport, symmetry energy

Collisions between heavy ions with large isospin asymmetries, made possible by the recent radioactive beam developments, represent a very efficient way to probe the structure of nuclear-*EoS* (Equation of State) symmetry term. In particular the symmetry energy behavior is influencing very dissipative reaction mechanisms, such as fragmentation processes, leading to important effects on fragment composition.

In central heavy ion collisions at intermediate energies the spinodal decomposition has been proposed as a possible mechanism for fragment formation, see Ref.[1] for a recent review. According to this description, fragments should reflect the properties of the low density phase, where they are formed. In charge asymmetric systems, the isospin distillation, i.e. the formation of more symmetric fragments surrounded by a neutron richer dilute phase, takes place. Here we will focus on fragmentation in semi-peripheral collisions, where intermediate mass fragments (*IMF*) are mostly produced in the overlap zone (the *neck region*) between projectile-like and target-like fragments (*PLF/TLF*, the *spectator region*), [2, 3, 4, 5, 6, 7] [8, 9, 10, 11, 12, 13, 14, 15, 16, 17, 18, 19]. We will discuss the influence of the symmetry energy on the features of this fragmentation mechanism. The presence of a density gradient between the neck (low density) and the spectator (high density) regions affects the N/Z of fragments in a different way with respect to the spinodal decomposition mechanism [20, 21, 22]. Moreover since the isoscalar density gradients are ruling the isospin transfer through the density dependence of the symmetry energy, we see that measurements of isospin observables in semiperipheral collisions will directly probe the slope of the symmetry term around saturation, of large impor-

tance for the structure of neutron-rich nuclei [23].

We consider the reactions $^{58}\text{Fe} + ^{58}\text{Fe}$ (charge asymmetric $N/Z = 1.23$) and $^{58}\text{Ni} + ^{58}\text{Ni}$ (charge symmetric $N/Z = 1.07$). In fact in these collisions, due to the uniform N/Z distributions, we do not have isospin gradients initially. We show that the study of the full reaction dynamics and of the possible occurrence of density gradients is essential in order to understand the isospin dynamics. We will finally suggest the measurement of some correlations between *IMF* properties, like mass, isospin content and “alignment”, particularly sensitive to the reaction mechanism and the isospin transport.

To get an insight into the behavior of neutrons and protons in asymmetric matter one can consider the density dependence of neutron and proton chemical potentials: $\mu_q = \partial\epsilon(\rho_q, \rho_{q'})/\partial\rho_q$, $q = n, p$, ϵ being the energy density. We recall that this quantity contains all contributions to the energy per particle (kinetic, potential and symmetry energy). In Fig.1 we report the density dependence of the n, p chemical potentials below normal density, where we expect that fragment formation takes place [7], for a system with asymmetry $I = (N - Z)/A = 0.2$ and for two choices of the iso-*EoS*. We refer to an *asy - stiff EoS* when we consider a potential symmetry term that is linearly increasing with nuclear density. We refer to an *asy - soft EoS* when the potential symmetry term increases up to a saturation around normal density, and then eventually decreases [20, 21, 22].

Since particles move towards the minimum of the chemical potential, it is possible to observe that there exists a density window, roughly $\rho_0/2 \leq \rho \leq \rho_0$ from Fig.1, where neutrons and protons can move in opposite directions: protons move towards a higher density region while neutrons move towards a lower density region. This phenomenon, called *isospin migration* [21], causes a neck neutron enrichment, due to the density gradient between the low density neck region and the spectator matter. We

*On leave from HH-NIPNE and University of Bucharest, Romania.

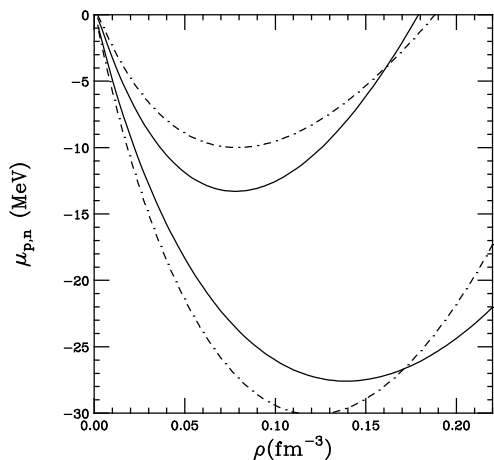


FIG. 1: Density dependence of the chemical potential for neutrons (upper curves) and protons (lower curves) for an asy-stiff (solid lines) and asy-soft (dashed lines) *EoS* with asymmetry parameter $I = 0.2$.

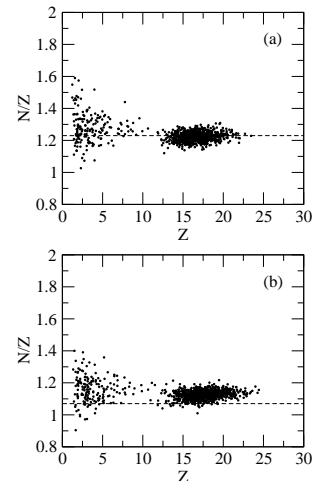


FIG. 3: Asymmetry vs. charge of each fragment arising from the simulation of the reaction $^{58}\text{Fe} + ^{58}\text{Fe}$ (a) and $^{58}\text{Ni} + ^{58}\text{Ni}$ (b) with an *asy-stiff EoS*. Horizontal dashed lines are the initial asymmetries of the colliding systems.

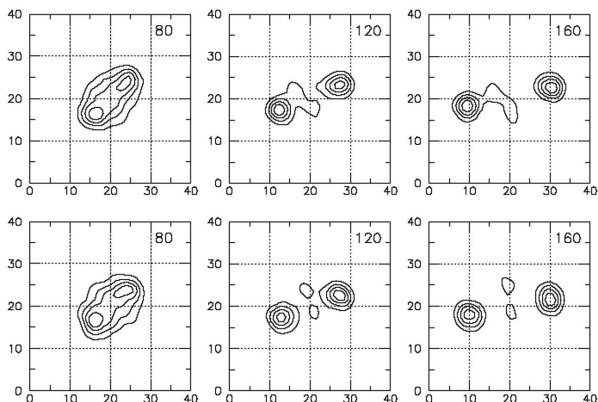


FIG. 2: Density contour plots on the reaction plane for two different events of the reaction $^{58}\text{Fe} + ^{58}\text{Fe}$ at 47 AMeV , $b_r = 0.5$. The box size is 40 fm . The numbers inside the box represent the time-steps in fm/c .

stress that this mechanism is different from the recently investigated isospin diffusion and N/Z equilibration processes in peripheral collisions [24, 25], that instead are due essentially to the presence of isospin gradients.

Reactions have been simulated by considering a stochastic extension of the microscopic transport equation *BNV* (Boltzmann-Nordheim-Vlasov), following a test-particle evolution on a lattice [26, 27, 28]. We consider a beam energy of 47 AMeV , and reduced impact parameter $b_r \equiv b/b_{max} = 0.5$ (semiperipheral). Using the *asy-stiff EoS* 40% of the events produce at least one *IMF* in the neck region (*ternary events*). In Fig. 2, density contour plots on the reaction plane are presented for two different events coming from the reaction $^{58}\text{Fe} + ^{58}\text{Fe}$ ($b_r = 0.5$, 47 AMeV).

The first row shows an event in which a fragment forms with a time delay and in a space region correlated to a target-like nucleus, unlike the event in the second row, which shows a rapid fragment formation in a region that is not correlated to any spectator remnants. Thus fragments are formed according to a variety of mechanisms and we will see how this influences their properties.

Fig. 3 reports the N/Z ratio of each fragment vs. the charge Z at the freeze-out time, obtained at the intermediate impact parameter $b_r = 0.5$.

The residual *PLF/TLF* nuclei (large Z range) show a different behavior in the two reactions: we note, in fact, that the points of Fe system are along the dashed line, that represents the initial system asymmetry, while for Ni reaction points lie above that line. The *IMF* (low Z range) behavior is similar for the two reactions: the points, for both reactions, lie above the dashed line, although for the reaction $^{58}\text{Ni} + ^{58}\text{Ni}$ the difference between the N/Z of *IMF*'s and large *PLT/TLF* residues seems to be less pronounced.

For a better understanding of Fig.3, we have to consider what happens during the pre-equilibrium phase [4, 29, 30, 31]. The asymmetry of the di-nuclear neutron-rich system changes from 1.23 (initial value) to 1.22 (at $t = 100 \text{ fm}/\text{c}$, instant in which fragments start to form) since 14 neutrons and 11 protons are evaporated, while the di-nuclear neutron-poor system changes from 1.07 to 1.12 as a consequence of a larger proton evaporation, due to the Coulomb repulsion (it loses 13 protons against 12 neutrons), becoming an asymmetric system. We can conclude that:

i) In the neutron rich reaction, the neutron emission due to pre-equilibrium goes in the same direction of the neck neutron enrichment, caused by the isospin-migration. So finally we observe slightly more symmet-

TABLE I: Asymmetry evolution of the residual nuclei arising from binary and ternary events.

<i>systems</i>	$t = 0$	$t = 100fm/c$	$t = 200fm/c$
$^{58}Fe + ^{58}Fe$	1.23	1.22	1.23 <i>binary</i> 1.19 <i>ternary</i>
$^{58}Ni + ^{58}Ni$	1.07	1.12	1.17 <i>binary</i> 1.125 <i>ternary</i>

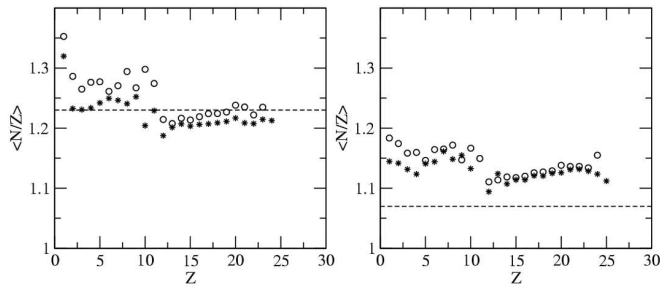


FIG. 4: Average asymmetry vs. Z for nuclei from the reactions $^{58}Fe + ^{58}Fe$ (left panel) and $^{58}Ni + ^{58}Ni$ (right panel) for an *asy-stiff* (circles) and *asy-soft* (triangles) *EoS*. Horizontal dashed lines represent initial asymmetry of colliding systems [21].

ric *PLF/TLF* residues accompanied by neutron-richer *IMF*'s;

ii) In the neutron-poor collision, the larger pre-equilibrium proton emission enhances the N/Z of the dinuclear composite system. The acquired asymmetry is then transferred to the neck region.

To better disentangle between the two mechanisms, one can study the charge composition of residues distinguishing between binary and ternary events (Table I).

For both reactions we note that the N/Z ratio of residual *PLF/TLF* nuclei in ternary events is lower than the value for binary events, since in the latter case the isospin-migration effect does not apply. The isospin dynamics effect is rather evident from the comparison with the asymmetry values at the end of the pre-equilibrium phase ($t = 100fm/c$ in the Table). For the $Fe + Fe$ system the N/Z of residues changes from 1.22 to 1.19, in ternary events; for the $Ni + Ni$ reaction this difference is not so evident (from 1.12 to 1.125) because the isospin-migration competes with proton evaporation. On the other hand, in binary events, we note the neutron enrichment of residues in the Ni reaction, due to a favorite proton pre-equilibrium emission.

In Fig. 4 the average asymmetry of products arising from the two reactions is shown for the two choices of the symmetry energy parameterization, *asy-stiff* and *asy-soft EoS*.

We note that fragments are more symmetric in the *asy-soft* case. This difference can be explained with the dif-

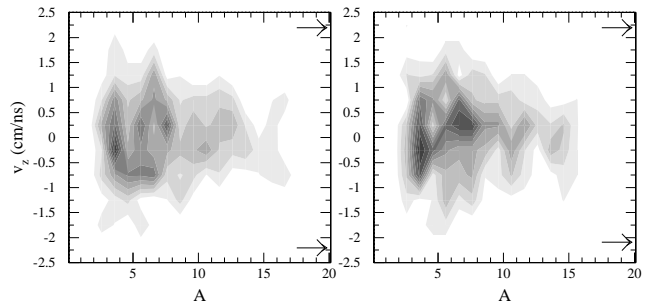


FIG. 5: Contour plots of the parallel velocity-mass distribution for the two systems: $^{58}Fe + ^{58}Fe$ (left) and $^{58}Ni + ^{58}Ni$ (right). Arrows indicate the positions of average PLF and TLF parallel velocity.

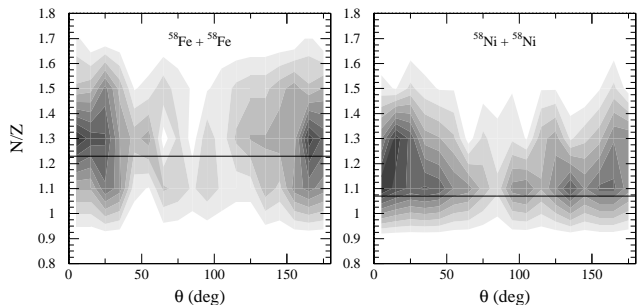


FIG. 6: Contour plots of the N/Z distribution versus the emission angle. *Asy-stiff* choice.

ferent behavior of the chemical potential in the two *EoS*, see Fig. 1, that will induce a different isospin-migration effect. For an *asy-soft EoS*, the proton chemical potential varies not so much in the region where the fragments form (from 0.08 to 0.15 fm^{-3}), while for neutrons there is a significant slope (however smaller than in the *asy-stiff* case). Therefore neutron enrichment of the neck will still cause an increase of the fragment asymmetry, but this increase will be smaller than in the *asy-stiff* case, where protons can even migrate out of the neck region. The fact that the N/Z of large fragments is smaller in the *asy-soft* case is due to pre-equilibrium effects, since with the *asy-soft EoS* more neutrons are emitted due to the more repulsive mean field below normal density, [20, 21, 22, 31]. On the other hand, the larger difference between *IMF* and *spectator* fragment asymmetries with the *asy-stiff* parametrization is a consequence of a more effective isospin migration, see the recent [33].

It is interesting to look also for some correlations between asymmetry, mass, velocity and direction of the outgoing fragments. As we will show, in this way we can even disentangle between features just related to the reaction mechanism and observables more sensitive to the isospin dynamics and symmetry energy.

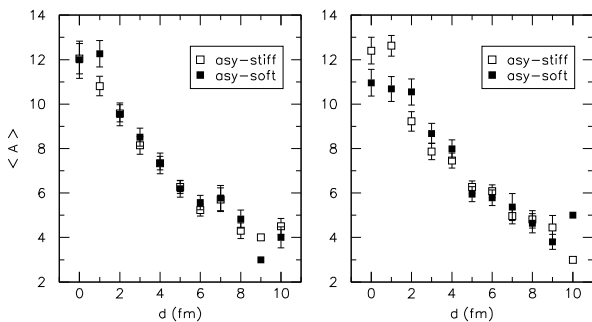


FIG. 7: Average IMF mass as a function of the distance from the $PLF-TLF$ axis at the freeze-out time for $47 AMeV$, $b_r = 0.5$ collisions. Left panel: $Fe + Fe$. Right panel: $Ni + Ni$. Empty squares: $asy-soft$ symmetry term. Full squares: $asy-stiff$.

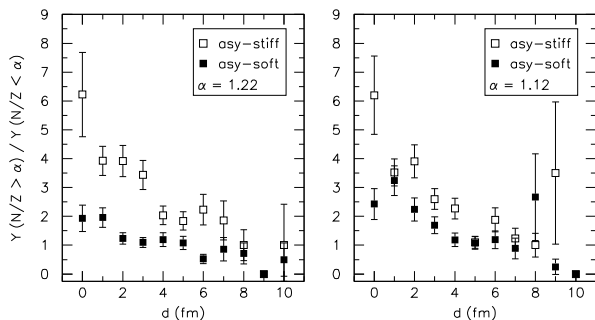


FIG. 8: Ratio of the IMF yields, with N/Z larger and smaller than the value α obtained just after pre-equilibrium emission, as a function of the distance from the $PLF-TLF$ axis at the freeze-out time for $47 AMeV$, $b_r = 0.5$ collisions. Left panel: $Fe + Fe$. Right panel: $Ni + Ni$. Empty squares: $asy-stiff$ symmetry term. Full squares: $asy-soft$.

In Fig.5 we present the behavior of the velocity along the beam direction versus the IMF mass. Lighter fragments are emitted at all angles and they have larger velocities with respect to more massive IMF 's that are more correlated to the spectator matter and are emitted on longer time scales.

The analysis of the N/Z distribution versus the emission angle (see Fig.6) reveals that larger fluctuations are present close to forward and backward angles. This indicates that IMF 's more correlated to the spectator matter may become more neutron-rich, since they interact for a longer time with the system and the isospin transport mechanism becomes more effective.

The presence of correlations between mass, neutron content and kinematical observables can be better evidenced by studying IMF properties vs. the ‘‘alignment’’, i.e. as a function of the distance d from the $PLF-TLF$ axis at the freeze-out time.

In Fig.7 we plot the behavior of the IMF average mass vs. the distance d for the n-rich ($FeFe$, left panel) and

the n-poor ($NiNi$, right panel) collision. The calculation is performed with the two choices of the density dependence of the symmetry term. In both cases we see a clear increase of the IMF masses with the fragment ‘‘alignment’’, independent of the stiffness of the used $Iso-EoS$. This appears a rather general feature of the *neck-fragmentation* mechanism: light fragments are emitted at earlier times and are not much driven by the spectator residues (PLF/TLF) [7]. This is also in line with the fact the light fragments may reach larger velocities (see Fig.5).

As a consequence we would expect a different amount of isospin migration vs. the IMF alignment, and now such correlation should be $Iso-EoS$ dependent. In Fig.8 we report the ratio of the IMF yields with the N/Z larger and smaller than the value, α , reached just after pre-equilibrium emission (see Table I), plotted vs. the alignment distance d at freeze out. For both systems we have a nice increase of the neutron enrichment with the alignment. As expected from the previous discussion on the physics of the *isospin migration*, the effect is more evident in the $asy-stiff$ choice.

We stress again that *neck-IMF*'s always present a neutron enrichment, *even in the case of a n-poor system*. The latter paradox is due to the pre-equilibrium isospin dynamics. In fact, as anticipated above, due to pre-equilibrium emission, the system will loose some protons and acquire a N/Z larger than the initial one. Then, before the di-nuclear system reseparates, the neutron excess is transferred to the neck region that is at lower density. Both effects, fast proton emission and neutron transfer, are connected to the symmetry term of the EoS . Some evidence has been found in recent data on ^{58}Ni induced fragmentation [15, 16, 32].

In conclusion, we have shown that isospin dynamic processes appear even in systems with initially uniform spatial asymmetry distribution, such as $^{58}Fe + ^{58}Fe$ and $^{58}Ni + ^{58}Ni$. From a chemical point of view, we do not expect N/Z gradients which can induce asymmetry variations. These variations are instead caused by density gradients during the reaction dynamics since the symmetry term of the EoS introduces a different behavior of the chemical potentials for neutrons and protons with respect to density. So, when the collision happens, the spatial distribution of the isoscalar density will induce variations even in the isovector density.

We have revealed an interesting correlation, typical of the *neck-fragmentation* mechanism, between IMF masses and corresponding alignment to the axis joining the $PLF-TLF$ residues. This suggests a time-hierarchy in the mid-rapidity fragment production with the lighter clusters formed at earlier times. When we combine to the isospin migration dynamics, an $Iso-EoS$ sensitive observable results to be the correlation between the neutron excess of IMF 's and the relative alignment.

The reactions $^{58}Fe + ^{58}Fe$ and $^{58}Ni + ^{58}Ni$ have been studied experimentally, focussing on central collisions and adopting a statistical description of multifragmen-

tation in [34, 35], or in semi-peripheral collisions in [15]. Asymmetry effects, as the ones described here, have been noted in [15], even in the second system. In this paper we suggest new interesting correlation analyses that can be pursued selecting semi-peripheral events and that ap-

pear particularly appropriate in order to investigate the isovector structure of the EOs as well as to shed some lights on the mechanism responsible for fragment production.

-
- [1] Ph.Chomaz, M.Colonna and J.Randrup, *Phys.Rep.* **389** (2004) 263-440.
- [2] G.F.Bertsch, D.Mundinger, *Phys.Rev.* **C17** (1978) 1646.
- [3] M.Colonna, N.Colonna, A.Bonasera, M.Di Toro, *Nucl.Phys.* **A541** (1992) 295.
- [4] L.G.Sobotka, *Phys.Rev.* **C50** (1994) 1272R.
- [5] L.G.Sobotka et al., *Phys.Rev.* **C55** (1997) 2109.
- [6] M.Colonna, M.Di Toro, A.Guarnera, *Nucl.Phys.* **A589** (1995) 160.
- [7] V. Baran, M.Colonna, M.Di Toro, *Nucl.Phys.* **A730** (2004) 329.
- [8] G.Casini et al., *Phys.Rev.Lett.* **71** (1993) 2567.
- [9] A.Mangiarotti et al., *Phys.Rev.Lett.* **93** (2004) 232701.
- [10] C.P.Montoya et al., *Phys.Rev.Lett.* **73** (1994) 3070.
- [11] J.Toke et al., *Phys.Rev.Lett.* **75** (1995) 2920.
- [12] J.Lukasik et al., *Phys.Rev.* **C55** (1997) 1906.
- [13] T.Lefort et al., *Nucl.Phys.* **A662** (2000) 397.
- [14] F.Bocage et al., *Nucl.Phys.* **A676** (2000) 391.
- [15] P. Milazzo et al., *Phys.Lett.* **B509** (2001) 204.
- [16] L.Gingras et al., *Phys.Rev.* **C65** (2002) 061604.
- [17] B.Davin et al., *Phys.Rev.* **C65** (2002) 064614.
- [18] J.Colin et al., *Phys.Rev.* **C67** (2003) 064603.
- [19] A.Pagano et al., *Nucl.Phys.* **A734** (2004) 504c.
- [20] M.Di Toro et al., *Prog.Part.Nucl.Phys.* **42** (1999) 125.
- [21] V.Baran et al., *Nucl.Phys.* **A 703** (2002) 603.
- [22] V.Baran, M.Colonna, V.Greco, M.Di Toro, *Phys.Rep.* **410** (2005) 335.
- [23] R.J.Furnstahl, *Nucl.Phys.* **A732** (2002) 24.
- [24] M.B.Tsang et al., *Phys.Rev.Lett.* **92** (2004) 062701.
- [25] G.Souliotis et al., *Phys.Lett.* **B588** (2004) 35.
- [26] G.F.Bertsch and S.Das Gupta, *Phys.Rep.* **160** (1988) 189.
- [27] A.Guarnera, *TWINGO code*, Ph.D. Thesis, Univ. Caen, July 1996.
- [28] V.Greco, A.Guarnera, M.Colonna and M.Di Toro, *Phys.Rev.* **C59** (1999) 810.
- [29] M.Farine et al., *Z.Phys* **A339** (1991) 363.
- [30] P.Danielewicz and Q.Pan, *Phys.Rev.* **C46** (1992) 2002.
- [31] Bao-An Li, C.M.Ko and Zhongzhou Ren, *Phys.Rev.Lett.* **78** (1997) 1644.
- [32] R.Moustbchir et al., *Nucl.Phys.* **A 739** (2004) 15.
- [33] V.Baran et al., *Isospin Transport at Fermi Energies*, arXiv:nucl-th/0506078.
- [34] D.V.Shetty et al., *Phys.Rev.* **C68** (2003) 021602R, D.V.Shetty et al., *Phys.Rev.* **C70** (2004) 011601R.
- [35] D.V.Shetty et al., *Phys.Rev.* **C71** (2005) 024602.